Comparison between ASTM D7205 and CSA S806 Tensile-Testing Methods for Glass-Fiber-Reinforced-Polymer (GFRP) Bars

Brahim Benmokrane,[1] Claude Nazair,[2] Xavier Seynave,[3] and Allan Manalo[4]

[1]**Corresponding author.** Professor of Civil Engineering and Tier-1 Canada Research Chair in Advanced Composite Materials for Civil Structures and NSERC Chair in FRP Reinforcement for Concrete Structures, Department of Civil Engineering, University of Sherbrooke, Quebec, Canada, J1K 2R1. Tel.: 1-819-821-7758.

Brahim.Benmokrane@usherbrooke.ca

[2]Professional Engineer,

Infrastructure Materials Laboratory

Ministry of Transportation of Quebec, Quebec City, Québec, Canada G1P 3W8

claude.nazair@mtq.gouv.qc.ca

[3]Quality Systems Engineer,

Pultrall, Thetford Mines, Quebec, Canada G6G 6Z5

xavier.seynave@pultrall.com

[4]Senior Lecturer,

Centre for Future Materials, Faculty of Health, Engineering and Sciences,

University of Southern Queensland, Toowoomba, Queensland 4350, Australia

Allan.Manalo@usq.edu.au

Abstract

The American Society of the International Association for Testing and Materials (ASTM) D7205 / D7205M-06 and the Canadian Standards Association (CSA) S806 contain the commonly used test methods for characterizing the tensile properties of glass-fiber-reinforced-polymer (GFRP) bars for use as reinforcement in concrete structures. These two standards, however, use different anchor dimensions and loading rates, thereby possibly yielding different properties for the same type of FRP bars. This paper assessed the results of a four-laboratory testing program comparing the sample preparation methods and test results according to ASTM D7205 and CSA S806. Each laboratory tested at least 10 samples prepared according to the recommendations in Annex A of the ASTM standard, and Annex B of CSA S806. Each type of sample was prepared by a single laboratory in order to minimize variation among the test specimens. The results show a statistically significant difference between the tensile strength measured using the CSA and ASTM provisions. Regardless of specimen preparation, the modulus of elasticity of the GFRP bars was the same with both test standards, but the ASTM standard returned a wider variation than the CSA.

Keywords: GFRP reinforcing bars; tensile test; ASTM; CSA; tensile strength; modulus of elasticity.

Introduction

Fiber-reinforced-polymer (FRP) bars have attracted significant interest as internal reinforcement in concrete structures due to their excellent corrosion resistance, light weight, high mechanical properties, and neutrality to electrical and magnetic disturbances. The results of several experimental studies, establishment of materials specifications, publication of design codes and guidelines, and the successful field applications in concrete structures (Benmokrane et al. 2006; Manalo et al. 2014) have driven the worldwide use and acceptance of FRP bars. Some of the successful applications of FRP bars as internal reinforcement in concrete structures include beams (Maranan et al. 2015), columns (Maranan et al. 2016), and slabs (Bouguerra et al. 2011). Carvelli et al. (2009) and Castro and Carino (1998) indicated that, when FRP bars are used as reinforcement in concrete structures, bar tensile strength and modulus of elasticity are the most important factors in design and use. These properties are also necessary for quality control and product specification (Kocaoz et al. 2005). That notwithstanding, bar manufacturers may specify different tensile properties even for the same type of FRP bars due to the difficulty in obtaining these properties by laboratory testing. In particular, assessing FRP-bar tensile properties is difficult because the bar must be adequately anchored to the testing machine to minimize stress concentration.

Micelli and Nanni (2004) suggested that the physical and mechanical properties of FRP bars be determined according to the prescribed test standards and methods. Moreover, Gentry et al. (2012) indicated that the appropriate test methods, along with the design guidelines and material specifications, provide engineers with the technical basis to design concrete structures with composite materials. As a result, a number of international standards have been drafted that prescribe the specimen preparation and testing method to properly determine the tensile properties of FRP bars. The International Organization for Standardization (ISO) 10406-1 (2015) is one of the recently drafted standards for FRP bar characterization. This standard provides the recommended length of the gauge section and suggests that an appropriate anchorage length should be used to effectively transmit the tensile force from the grip to the bar. Castro and Carino (1998) highlighted the use of acceptable specimen dimensions to effectively characterize the tensile properties of FRP bars. The American Society of the International Association for Testing and Materials (ASTM) D7205 / D7205M-06 (2011) and the Canadian Standards Association (CSA) S806 (2012) have standardized the specimen preparation and procedures for assessing the quasi-static longitudinal tensile strength and elongation properties of FRP bars. These two standards, however, prescribe different anchor dimensions and loading rates for characterizing the tensile properties of FRP bars, which might yield different measured properties. Thus, it is important to assess the efficiency and reliability of ASTM D7205 / D7205M-06 (2011) and CSA S806 (2012), as they are the tensile-test methods commonly used for material specifications, research and development, quality assurance, and design and analysis of FRP bars as reinforcement in concrete structures.

This paper assessed the results of a four-laboratory testing program comparing the sample preparation methods and results for the tensile testing of No. 6 sand-coated GFRP bars (19 mm nominal diameter) according to ASTM D7205 and CSA S806. Each laboratory was provided with at least 10 samples prepared as per the recommendations in Annex A of ASTM D7205 and in Annex B of CSA S806. Each type of sample was prepared by a single laboratory in order to ensure a lower level of variation for this operation. Theoretical and statistical analyses of the test data were then conducted to assess the variability of the tensile strength and modulus of elasticity (MOE) of the GFRP bars measured according to these two test standards.

ASTM and CSA Tensile-Test Methods for FRP Bars

ASTM D7205 / D7205M-06

ASTM D7205 / D7205M-06 (2011) is used to determine the quasi-static longitudinal tensile strength and elongation properties of FRP composite bars used as tensile elements in reinforced, prestressed, or post-tensioned concrete. In this test method, the FRP bar is preferably fitted with anchors before mounting in a mechanical testing machine. The anchors should be designed in such a way that the full tensile capacity can be achieved without slip throughout the length of the anchor during the test. This test standard recommends at least five specimens per test condition.

The ASTM standard stipulates that the overall specimen length and gauge length shall be the free length plus two times the anchor length. The free length between the anchors L shall not be less than 380 mm nor less than 40 times the effective bar diameter d. In conducting the test, the speed of testing shall be set to a constant strain rate so as to produce failure within 1 to 10 min from the outset of load application. The suggested rate of loading is a strain rate of 0.01/min or a nominal cross-head speed of 0.01/min times L. An extensometer can be attached to the bar to measure strain and to calculate the tensile modulus of elasticity. The ASTM standard recommends calculating MOE within the lower half of the stress–strain curve, with the start point being a strain of 0.001 and the end point being a strain of 0.003.

The specimen preparation detailed in Annex A stipulates that the anchor shall be provided to ensure that bar failure occurs outside of the anchor and to prevent excessive bar slip prior to tensile failure. A steel tube with an outside diameter of 48 mm, a wall thickness of at least 4.8 mm, and an anchor length L_a of at least 460 mm is recommended for adequate anchoring of the 19 mm diameter FRP bar. It is also highly recommended to use a polyvinyl chloride (PVC) cap with a concentric through hole to center the FRP bars inside the steel tube. The tube may be filled with either polymer resin or expansive cement grout that is compatible with the resin used in manufacturing the FRP bars. A threaded steel plug is screwed on to tube to contain the resin or grout. The anchor filler materials are then allowed to cure before the testing. These recommendations are limited to FRP bars that require less than 400 kN to fail.

CSA S806-12

Annex B of CSA S806 (2012) specifies the requirement for an anchor for FRP bars to be tested under tensile loading of not greater than 300 kN. This standard recommends using a steel tube with a wall thickness of at least 5 mm and an inner diameter of 10 to 14 mm greater than the bar diameter. The length of the steel-tube anchor (same as L_a) shall be at least equal to $f_u A/350$, but not less than 250 mm, where f_u is the bar ultimate tensile strength and A is the nominal cross-sectional area. Similarly to the ASTM standard, the CSA standard recommends the use of resin or non-shrink cement grout with properties compatible with the matrix used in manufacturing the FRP bar. The specimen length must be at least $40d+2L_a$.

Annex C in CSA S806 (2012) specifies the test method for determining the tensile properties of FRP bars. The test procedures specified in this annex are very similar to that of the procedures recommended in ASTM D7205 / D7205M-06 (2011), except for the rate of loading and the calculation of the modulus of elasticity. The CSA standard specifies that the tensile loading be applied at a stressing rate of 250 MPa to 500 MPa/min. Similarly, the tensile MOE should be measured between 25% and 50% of the FRP-bar failure strength. Table 1 summarizes the differences between the ASTM and CSA standards.

Experimental Program

Materials

Grade II (standard modulus) and sand-coated No. 6 GFRP bars made of continuous glass fibers impregnated in a vinyl-ester resin through the pultrusion process were used in this study. All samples were taken from the same production lot (lot number 116003) of straight

V-Rod 20M standard bars. The bar nominal diameter and cross-sectional area were 19.0 mm and 286.5 mm^2, respectively. Table 2 summarizes the physical properties of the GFRP bars determined according to the appropriate ASTM test standards. The actual bar diameter and cross-sectional area as measured using the immersion cross-sectional area test according to CSA-S806 (2012), Annex A, are also reported in Table 2.

Specimen Details and Preparation

A total of 48 specimens were prepared according to the provisions of ASTM D7205 (hereafter ASTM specimens), while 40 were prepared according to CSA S806 (hereafter CSA specimens). Figure 1 shows the details of the tensile-test specimens. The ASTM specimens had a gauge length of 870 mm or almost 46*d*. Similarly, a steel anchor was prepared according to the minimum dimensions recommended in Table A1.1, ASTM D7205 (2011), i.e., L_a = 460 mm, outside diameter D_o of 48 mm, and inside diameter D_i of 38 mm. On the other hand, the CSA specimens had a gauge length of 760 mm or exactly equal to the recommended minimum of 40*d*. A steel tube with an outside diameter D_o of 42 mm, inside diameter D_i of 32 mm, and L_a = 675 mm was used for the CSA anchor. This resulted in total length of 2110 mm and 1790 mm for the CSA and ASTM standards, respectively. The steel tubes used were Schedule 80S and had a yielding stress of 205 MPa. The anchor prepared according to ASTM D7205 was larger but shorter than that according to the CSA standard. It should be noted that the diameter of steel tube recommended in the ASTM standard is the same for bars 19 mm to 25 mm in diameter. Table 3 provides a summary of the specimen dimensions for both standards. These specimens were equally and randomly distributed among the four laboratories. It is important to note that all the ASTM specimens were prepared by Laboratory C and all the CSA specimens by Laboratory B. This division of production was opted for because it is difficult to fabricate all of the specimens needed at the same time. It is important to note, however, that both laboratories used the same procedure, grout, and steel tube. The next section provides more details about the different testing laboratories.

When the specimens were prepared, each FRP bar was centered and aligned inside a steel tube through a 3 mm thick polyvinyl chloride (PVC) washer with a concentric hole. The washers were machined to fit tightly in the steel tube. Expansive cement grout supplied by RockFrac was used as a filler material for both anchor types. A single batch of grout was prepared for each specimen type to eliminate any differences in grout properties. Prior to pouring the grout, the inner surface of the tube was cleansed with acetone to remove any impurities that might affect adhesion between the grout and tube. Wooden formwork was used to keep the steel tubes and the FRP bars in the vertical position. The cement grout was prepared and poured into the steel tubes with a narrow spout. It was then allowed to cure for 24 h before it was flipped to cast the other anchor. Figure 2a shows the actual specimens ready for testing

Test Laboratories and Setup

Bar testing was conducted at 4 facilities, i.e., an independent testing laboratory, bar manufacturer, asset owner, and university. These testing facilities were designated as A, B, C, and D, respectively. Table 4 lists the test machine, strain-acquisition device, and loading rate used by each testing facility. All of the test machines had a capacity of 2000 kN, in compliance with ASTM E4 (2001), and were newly calibrated to ensure the accuracy and reliability of the measured data. Since Laboratory C was unable to use the strain rate as a means to control the machine during the tests, a constant cross-head speed of 8.7 mm/min was used instead. The average speed of testing in MPa/min adopted by Laboratory C was then measured after the test between the calculations points of the modulus and reported in the below table.

The tensile tests were conducted according to ASTM D7205 / D7205M-06 (2011) and CSA S806-12, Annex C. All of the specimens were carefully handled to avoid bending and twisting, and placed to in the test machine for proper alignment. Each specimen was instrumented with a strain-acquisition device to record specimen elongation during testing (Figure 2b). These instruments were detached from the specimen when the load reached 75% of the estimated ultimate load to avoid damage. The applied load and bar elongation were electronically recorded during the test with a computerized data-acquisition system.

Results and Discussion

Tables 5 and 6 summarize the results of the tensile testing. The nominal cross-sectional area of the GFRP bars was used to calculate the tensile strength and MOE, as seen in Tables 5 and 6, respectively.

Ultimate Tensile Strength

All of the specimens exhibited linear-elastic behavior up to failure and failed suddenly, as expected, due to tensile-fiber rupture at the gauge length. Prior to failure, a popping noise was heard, caused by some of the fibers and/or the resin failing on the outer perimeter of the bar. No slip was observed in any of the tested specimens. Figure 3 shows the typical failure. The highest failure load recorded was 295.3 kN (940 MPa), which is within the maximum recommended failure load by the ASTM and CSA. The ultimate tensile strength was calculated according to both the ASTM and CSA standards by dividing the maximum load at failure to bar nominal cross-sectional area. Table 5 lists the tensile strength calculated for the ASTM and CSA specimens. It should be noted that each laboratory was required to test only 10 specimens but Laboratory A tested 11, and Laboratories C and D tested all 12 ASTM specimens.

Table 5 shows that the tensile strength of the GFRP bars measured according to ASTM D7205 ranged from 435 MPa to 933 MPa, while those measured according to

CSA S806 ranged from 835 MPa to 940 MPa. The test results also reveal that the tensile strength of the six ASTM samples (results flagged with an asterisk) is significantly inferior to the overall average strength. These results could be discarded because they are far from the average strength and the material's recognized tensile strength. Since the results could be construed as a proof that the material might be defective, they have been reported and were taken into account in the statistical analyses. Moreover, the average strength of the ASTM samples is lower than the average strength of the CSA samples. The standard deviation is also respectively higher. The measured strength values of the CSA specimens are remarkably consistent with the coefficient of variation (COV) of less than 5%, which is extremely encouraging. On the other hand, the COV of the ASTM specimens is 16%. Discarding the outliers from the analysis would still result in a lower average tensile strength for the ASTM specimens (866.5 MPa) compared to the CSA specimens (899.4 MPa) and a COV of 4.5%.

Modulus of Elasticity

The tensile MOE of the GFRP bars was calculated according to the requirements of each standard. For the ASTM specimens, the MOE was calculated from the slope of the stress–strain curve between 0.1% and 0.3% of strain, while, for the CSA specimens, it was calculated from the slope of the stress–strain curve between 25% and 50% of the maximum tensile strength. It is important to note that, in both methods, the MOE is calculated by linear regression of the stress–strain curve, instead of the average value between two isolated points. Figure 4 shows the typical stress–strain behavior of a GFRP bar. It also shows the location wherein the MOE was calculated for both ASTM and CSA method. The calculated MOEs were then listed in Table 6. It should be noted that there was no extensometer slippage for this strain interval.

Table 6 shows that the MOE of the ASTM specimens ranged from 45.01 GPa to 77.35 GPa, while the CSA specimens ranged from 51.84 GPa to 62.22 GPa. The wide range of

MOE values for the ASTM specimens can be due to the recommended calculation method. It should be noted that the interval used in the ASTM standard is shorter than the CSA one and is located closer to the start of the test, when the testing machine and its components may not be acting evenly on the sample because of temporary slippage and play, which need to be compensated for. Such movements broke the linearity of the recording and led to erroneous calculations of the slope of the stress–strain graph leading to off-the-chart MOE values (flagged with an asterisk) were probably caused by these undesirable extensometer movements. An example would be Test No. 5 in Laboratory A, in which an MOE of 77.35GPa was measured, probably due to this undesirable movement. Nevertheless, the MOE values measured for the FRP bars across the testing program were almost the same. This is due to this property calculated based on the data obtained when the relationship between the stress and strain was linear. In this level of load, the bar mechanical properties are dominated by the elastic properties of the fibers and resin.

Loading Rate

Li et al. (2015) indicated that the different loading rates can result in different tensile-strength properties obtained from the testing of FRP bars. This is one reason why different researchers and manufacturers have reported mixed results even for the same bar type. They further indicated that the tensile strength increased as did the loading rate (from 2 mm/min to 6 mm/min), but became constant when tested at a loading rate higher than 6 mm/min. This is due to the time-dependent (rate) of the viscoelastic matrix material. At high loading rates, the resin can effectively transfer the stress from the periphery to the center of the GFRP bar, leading to better load sharing and higher tensile strength than low loading rates. As the loading rates adopted in this study was around 8.7 mm/min for all specimens, this parameter cannot be considered a major factor governing the difference between the tensile strength of GFRP bars measured according to the ASTM and CSA standards. Li et al. (2015) also found that the loading rate had limited effects on the elastic modulus of GFRP bars as this property is calculated at the linear range of the stress–strain data. This finding was further confirmed in our study, since both the ASTM and CSA test methods returned almost the same modulus values. We noted, however, more variation with the ASTM test method than the CSA one, most probably because of poorer stability of the test system as a whole (hydraulics, grips, extensometer, or the Linear Variable Differential Transformer (LVDT)) in the strain intervals considered in calculating the modulus. While both standards basically require a steady strain rate or load rate during the entire loading regime, ASTM recommends calculating the modulus as between 0.1% and 0.3% of the strain, while CSA recommends using 25% and 50% of the ultimate load. Table 7 provides the actual loading rate at the beginning and end, as well as the average over the recommended interval for modulus calculation. The values listed inside the parenthesis are the standard deviations of the results. It is important to note that all specimens failed within 3 min of load application.

The table shows that the applied loading rates were well within the recommended stressing rate of 250 MPa to 500 MPa/min by CSA S806, except at the 0.1% strain for Laboratories B, C, and D. This result shows that it is very difficult to ensure a constant level of stress during the initial load application, which explains the high variation of the measured MOE using the ASTM approach. On the other hand, a more consistent loading rate was achieved at a higher load—i.e., between 25% and 50% of the ultimate—once the specimen and grips had settled properly. This resulted in less MOE variation for the CSA specimens. Laboratories A and B, with the ability to control the loading rate, clearly illustrate this. The loading rate was not constant with the ASTM test method between the start of the test (0.1%–0.3%) and the middle of the test (25%–50%). It increased by 2% at Laboratory A, 26% at Laboratory B, 11% at Laboratory C, and 13% at Laboratory D. Moreover, the difference between the loading rate at the start and end of the ASTM interval of strain used for modulus calculation can be as high as 37%. This difference is high enough to create problems in analyzing test data. Therefore, controlling the test machine by cross-head speed is not a satisfactory means of complying with the requirement of a constant strain/load rate. The closer to the start of the test, the more likely results can suffer from the effects of a slight slippage of the sample within the grips or the tightening of play in the mechanical assembly. This is heavily machine-dependent: Laboratory A's Instron machine is a brand-new, state-of-the-art piece of equipment and evidenced much less variation in the test conditions (although not in the test results) than any other testing machine. Laboratory B provided less variation than Laboratory D even though using the same Satec-Baldwin hardware but with a newer control unit.

Anchor Geometry

A variety of gripping systems have been developed to provide effective anchorage at the ends of the FRP bars in tension and to prevent premature failure. Castro and Carino (1997) developed a system involving embedding the bar ends in steel tubes with a high-strength gypsum-cement mortar. Similarly, Malvar (1995) designed special grips consisting of four aluminum blocks bolted together to characterize the tensile strength of different FRP bars. Tannous and Saasatmanesh (1998) adopted an anchor system consisting of coating both ends of the bar with a sand–epoxy mixture and then placing it in steel tube cut along its longitudinal axis to get two cylindrical shells. Schesser et al. (2014) highlighted that the key parameters for the effective design of all these gripping systems are grip length, steel-tube dimensions, and volume/thickness of the grout.

It should be noted that the ASTM specimens have a longer gauge length (870 mm) than the CSA ones (760 mm). These lengths are around 45 and 40 times the nominal diameter of the GFRP bars. Wisnom (1999) indicated that the strength of composite materials tended to drop with increasing volume of material. Castro and Carino (1997), however, found no statistically significant influence on the mean tensile strength of FRP bars with a free-length-to-diameter ratio of 40 to 70. Thus, it can be concluded that the gauge length did not produce the difference in the measured tensile strength between the ASTM and CSA specimens.

Another main difference between these specimens is the steel-anchor geometry, as indicated in Section 3.2. The ASTM specimens had an L_a = 460 mm, D_o = 48 mm, and D_i = 38 mm, while the CSA specimens had an L_a = 675 mm, D_o = 42 mm, and D_i = 32 mm. The ASTM also recommended a minimum wall thickness of 4.8 mm and grout space of 4 mm between the bar outer surface and the steel-tube inner wall. Both specimen types satisfied these minimum requirements. While the ASTM-recommended L_a is shorter than the CSA one, these anchorage lengths are suitable, as demonstrated by other researchers. Preliminary tests conducted by Kocaoz et al. (2005) indicated that an anchor length of 305 mm was sufficient for proper restraint of 12.5 mm diameter GFRP bars. An expeditious study by Castro and Carino (1998) suggested a minimum embedment length of 15 times the bar diameter, which is only 285 mm for 19 mm diameter bar. Schesser et al. (2014) recommended a minimum anchor length of 457 mm for a 19 mm diameter FRP bar with a nominal tensile strength of 900 MPa. Similarly, Li et al. (2015) found that a 300 mm long steel-tube anchor with an outer diameter of 54 mm and thickness of 6.5 mm filled with expansive cement is sufficient for 25 mm diameter FRP bars. While Portnov and Bakis (2008) suggested that a more uniform distribution of the applied shear stress near the grips can be achieved with anchors of sufficient length, there is not enough evidence to conclude that the higher tensile strength of the CSA specimens resulted from the longer anchor length than the ASTM specimens. Both specimen types exhibited the same failure behavior, i.e., fiber rupture within the gauge length with no observed bar–anchor slippage.

Zhang et al. (2001) indicated that, for FRP ground anchors, grout deformation decreased as did the grout cover. This restrains the rod and increases the anchor stiffness, resulting in increased load capacity. The thickness of the grout forming a cylindrical shell around the FRP bars was around 8.5 mm for the ASTM specimens and 6.5 mm for the CSA specimens. As highlighted in Section 4.2, the MOE of the ASTM and CSA specimens were almost the same, indicating that the grout thickness had an insignificant effect on the tensile stiffness of the FRP bars. This finding is supported by Schesser et al. (2014), who found that a grout thickness of around 10 mm is optimum to develop the maximum gripping pressure between the steel tube and the 20 mm diameter FRP bar.

Sample Surface Temperature

Portnov and Bakis (2008) indicated that the anchors should be designed to minimize stress concentrations in the composite bars to avoid premature shear failure. This was achieved with both the ASTM and CSA specimens by placing a steel tube filled with expansive cement grout around the ends of the bars. Li et al. (2015) found that the expansive cement is an optimum filler in the end anchorage for the tensile testing of FRP bars as they can distribute the loading force uniformly along the anchored length. The thickness of the grout around the sample is different, however, given the size difference between the anchors used in the ASTM and CSA standards. It is well-known that thick grout with a high cement content produces high temperature during curing due to heat of hydration. The surface temperature of the specimens during curing was measured to monitor the grout’s exothermal reaction. A thermocouple sensor was attached at mid-length of the bar surface, embedded in the grout and the steel anchor (Figure 5a). As noted, the anchors were filled with a same grout mix to ensure consistency between them. For this particular study, all the test specimens were prepared by Laboratory B under the same conditions. They all had the same level of curing and compressive strength as they were prepared at the same time by the same technician. The temperature was recorded simultaneously (1 record per minute) until the grout cooled down (see Figure 5b).

Figure 5b shows that the temperature rise in the grout was higher in the ASTM anchor: it reaches 202°C, with a 100°C rise in less than one minute. Material certification standards (like CSA S807) require a minimum glass transition temperature (Tg) of 100°C. The temperature inside the ASTM and CSA anchors was above this minimum for 34 min and 17 min, respectively. It is worth noting that the T_g measured for the GFRP bars (lot number 116003) was 125°C. The ASTM anchor exceeded this temperature for 23 min, but was not reached in the CSA anchor. Consequently, there was a risk of damaging the specimen when using a thicker grout. This result shows that the GFRP bars prepared according to the suggested ASTM procedures (Annex A) may experience a severe thermal ordeal, taking the bar surface temperature above its glass transition temperature.

It is well-known that the mechanical properties of FRP materials are susceptible to degradation at high temperature. Consequently, Robert and Benmokrane (2010) suggested that the design engineer should take into account the duration of time the FRP bars can withstand high temperature. Based on this study's experimental results, the average tensile strength of the ASTM bars was almost 10% lower than that of the CSA bars. These lower tensile-strength properties can be due to the bar being exposed to high temperatures as the cement grout cures. As noted in Table 1, the vinyl-ester resin used in manufacturing the FRP bars has a T_g of around 125°C. The high temperature to which the ASTM specimens were exposed reduced the force transfer between the fibers through the bond to the matrix, resulting in lower tensile strength than the CSA bars. Robert and Benmokrane (2010) made similar observations, reporting an almost 35% reduction in the tensile strength of 12.7 mm diameter GFRP bars subjected to a temperature of 200°C. Wisnom (1999) indicated that the outer fibers of FRP rods experienced higher stresses than inner fibers due to the shear lag effect. Thus, the exposure of the ASTM specimens to a temperature higher than the T_g of the GFRP bars may have decreased the tensile strength of the outer fibers, which initiated failure at a load lower than the CSA specimens. It should be noted that there were no indications anywhere in the test standards about avoiding the overheating of the FRP bars when large volumes of grout were used. Castro and Carino (1998) are probably the only researchers who suggested using sand to reduce the cement required and control the rise in temperature during curing. The authors had used approach in the past, but it was observed that bar slippage from the anchor was high and gave inconsistent results for bars with a tensile strength near 1000 MPa.

After testing, the end anchors of the specimens were carefully cut into halves to observe the condition of the bars embedded in the steel tube. Figure 6a shows some exposed fibers at the bottom of the ASTM specimens, indicating that the bar was locally damaged inside the anchor. The mode of failure appears to be interlaminar rupture similar to what can be observed after a short-beam shear test, which further indicates that the epoxy matrix is affected during curing. The loss of the bar’s sand coating can also be clearly seen. This explains the lower tensile strength of the GFRP bars prepared according to the ASTM method as the portion of the bars embedded in the steel tube had reduced mechanical properties due to the high temperature during curing. Figure 6b shows the condition of the FRP bars prepared and tested according to the CSA standard. Clearly, the coating at the bar end was damaged and chipped off, but there was no sign of fiber damage. This patently indicates that the CSA end anchorage both provided an effective grip of the tensile specimens and prevented any premature bar failure at the bar ends. It also constitutes a more cost-effective anchor system (anchors are not reusable) as the method calls for smaller steel tubes and less grout than for the ASTM specimens. The authors therefore suggest that users should consider Annex A of ASTM D7205 or other test standards as useful recommendations to facilitate testing of the FRP bars, but not as being mandatory, and recognize that any deviation in specimen preparation is permissible as long as it optimizes the reliability of the test results.

Theoretical and Statistical Analyses of Tensile Properties

This section presents the theoretical and statistical analyses to determine the variability of the tensile strength and MOE of the GFRP bars measured according to the ASTM and CSA standards.

Mix Rule

The theoretical values of the tensile strength and MOE of the GFRP bars were assessed using the mix rule in Equation (1) and reported in Table 8. The actual fiber-weight ratio of 82.7% (Table 2) and the longitudinal properties of the glass fibers and vinyl-ester resin reported by Roopa et al. (2014) were used to calculate the tensile properties:

$$P_{bar} = P_f v_f + P_m v_m \qquad (1)$$

where P_{bar} is the mechanical property of the FRP bar, P_f is the mechanical properties of the glass fibers, v_f is the fiber volume fraction, P_m is the matrix mechanical property, and v_m is the matrix volume fraction. A fiber weight ratio of 82.7%, glass-fiber density of 2.56 kg/m^3, and vinyl-ester density of 1.80 kg/m^3 give v_f = 0.77 and v_m = 0.23.

The comparison showed that the GFRP bars failed at a tensile stress much lower than their theoretical strength, i.e., 52.8% for the ASTM specimens and 57.9% for the CSA ones. Castro and Carino (1998) strongly emphasized that the mechanical properties of the FRP bars were highly influenced by fiber and matrix properties, fiber volume fractions, and the efficiency of stress transfer from the bar surface to inside fibers. Since the fibers, matrix, and fiber content were nearly the same for the GFRP bars tested, the difference in the measured properties can be attributed to the stress transfer among the fibers. The fact that the measured tensile strength of the GFRP bars was lower than the theoretically predicted value can be due to defects or the shear lag effect. It can also be due to the difficulty of keeping the glass fibers parallel to one another during the pultrusion process, as indicated by Carvelli et al. (2009). On the other hand, the measured MOE is only 2.0% to 3.3% higher than the theoretical value.

This is expected as bar mechanical properties are dominated by the elastic properties of the fibers and resin at lower loads. The tensile-strength properties are, however, measured just before final failure when the stress distribution along the fibers is already not uniform.

Data Analysis and Comparison

The data were analyzed with IBM Statistical Package for the Social Sciences (SPSS) Statistics 23.0 (2015) to compare the significance of the difference at a 95% confidence interval between the measured tensile strength and MOE of the GFRP bars. The independent samples *t*-test (or independent *t*-test) was used to compare the means of the tensile-strength test and the MOE between the ASTM and CSA specimens, while the one-way analysis of variance (ANOVA) was used to determine whether there were any significant differences between the properties measured at Laboratories A, B, C, and D.

The independent *t*-test of means in Table 9 show that the tensile strength of the ASTM specimens is significantly different from the CSA ones (*2-tailed sig.* is less than 0.05). The group-statistics table further shows that the GFRP bars tested according to CSA S806 had statistically significantly higher tensile strength (899.45 ± 26.52 MPa) than those obtained tested according to ASTM D7205 (819.80 ± 130.84), $t(83) = 3.78$, $p = 0.000$. The independent sample test also showed very high variation among the tensile strengths determined according to the ASTM test method. This holds true when the outliers according to the ASTM method (866.53 ± 38.88), $t(77) = 4.41$, $p = 0.010$ are discarded from the analysis. The one-way ANOVA in Table 10, however, shows that the average tensile-strength properties of the GFRP bars tested in all 4 laboratories according to either ASTM D7205 ($p = 0.270$) or CSA S806 ($p = 0.109$) were all equal. This is further confirmed with Tukey's HSD Post Hoc multiple comparisons in SPSS.

The independent samples *t*-test and Tukey's test for homogeneity of variances in Tables 11 and 12, respectively, reveal no significant difference between the variances of the

MOE measured with either the ASTM or CSA standard. The one-way ANOVA ($F(3,81) = 15.14$, $p = 0.000$) yielded a statistically significant difference in the MOE measured at the 4 laboratories. A Tukey's HSD Post Hoc test (Table 12) revealed that the average MOE measured in Laboratory B (51.9 ± 3.3 min, $p = .046$) was statistically significantly lower than that at Laboratory A (23.6 ± 3.3 min, $p = .046$), C (23.4 ± 3.2 min, $p = .034$) and D (27.2 ± 3.0 min). On the other hand, there were no statistically significant differences between Laboratories A and C ($p = 0.258$), A and D ($p = 0.839$), and C and D ($p = 0.733$). The higher deviations noted for Laboratories C and D were due to the lack of automated control of the testing machine's stress rate. The lower modulus recorded by Laboratory B was due to the initial gauge length being underestimated by 9%. Using the actual initial gauge length would give values much closer to those obtained at the other laboratories. No corrections were made to the figures in this paper in order to support the conclusions based on the original results. It is strongly recommended, however, that this parameter be properly measured to ensure more reliable MOE values from tensile testing.

Distribution and Guaranteed Tensile Properties

Kocaoz et al. (2005) highlighted the importance of defining the mean values and distribution of the tensile properties of FRP bars, which engineers could use for design purposes and composite manufacturers for quality control and optimization. Figures 7a and 7b show the distribution of the tensile strength and MOE, respectively of the GFRP bars tested according to both standards. The results reveal a wide distribution of tensile strength measured according to the ASTM standard, with some values even lower than 90% of the mean value (819.8 MPa). On the other hand, 90% of the bars tested according to the CSA standard were within ±5% of the mean value (899.4 MPa), while the other 10% were within the -10% of the mean value. The distribution of the MOE shown in Figure 7b indicates that the spread of the results for both standards was almost same. More than 55% and 62% of the tested bars have a measured MOE within ±5% of the mean value according to both the ASTM and CSA standards, respectively. One important thing to note, however, is that an almost 7% of the bars tested according to ASTM D7205 have an MOE of less than 10% from the mean value (55.71 GPa). This accounts for the ASTM method yielding higher COV values than the CSA method. More importantly, Carvelli et al. (2009) indicated that the output of the experimental tests and test repeatability are the only ways to guarantee the efficacy and reliability of the particular testing method. Therefore, the results from this study show that the CSA method provided better repeatability, as shown by the smaller dispersion of the tensile-strength values and MOE.

The guaranteed tensile properties are important for design purposes when FRP bars are used as reinforcement in concrete structures. These properties are the minimum values that have to be guaranteed by bar manufacturers for product certification. ACI 440.1R-15 (2015) provided equations to calculate the guaranteed tensile strength f^*_{fu} and modulus of elasticity E_f of FRP bars, as shown in Equations (3) and (4), respectively.

$$f^*_{fu} = f_{u,ave} - 3 \cdot SD \qquad (3)$$

$$E_f = E_{f,ave} \qquad (4)$$

where $f_{u,ave}$ and $E_{f,ave}$ are the mean tensile strength and modulus of elasticity, respectively, and SD is the standard deviation of the test results. CSA S807-10 (2010) indicates that the guaranteed properties be calculated with these equations:

$$f^*_{fu} = F_{t\_CSA} \cdot f_{u,ave} \qquad (5)$$

where $F_{t\_CSA} = (1\text{-}1.645 \cdot COV)/(1+(1.645 \cdot COV/n^{1/2}))$, COV is the coefficient of variation of the test results, and n is the number of specimens. Similarly, the specified values for the MOE from tests are determined as follows:

$$E_f = F_{E\_CSA} \cdot E_{f,ave} \quad \text{if } COV \geq 5\% \qquad (6)$$

where $F_{E\_CSA} = (1\text{-}1.645 \cdot COV)/(1+(1.645 \cdot COV/n^{1/2}))$

$$E_f = E_{f,ave} \qquad \text{if } COV < 5\% \qquad (7)$$

Table 13 provides the guaranteed tensile strengths and MOE of the GFRP bars obtained according to ACI 440.1R-06 and CSA S807-10. The guaranteed tensile strength of the GFRP bars determined according to ACI 440.1R-06 is 427.9 MPa, compared to 819.9 MPa as determined by the ASTM and CSA standards, respectively. On the other hand, the guaranteed tensile strength is 581.8 MPa and 849.3 MPa according to the ASTM and CSA standards, respectively, based on CSA S807-10 recommendations. Banibayat and Patnaik (2014) highlighted that the difference in the guaranteed properties yielded by ACI 440.1R-06 and CSA S807-10 are due to different philosophies adopted by these design standards. They also indicated that ACI 440.1R underuses test values compared to CSA S807 in determining guaranteed values. Regardless of the calculation method, the CSA specimens gave a higher guaranteed tensile properties than the ASTM specimens. If the outliers are discarded from the analysis, the ASTM specimens would have a guaranteed tensile strength of at least 749.8 MPa. Similarly, the guaranteed MOE are 55.7 GPa and 56.4 GPa according to the ASTM and CSA standards, respectively. That notwithstanding, an E_f of only 46.8 GPa can be specified for the ASTM specimens if calculated according to CSA S807-10 recommendations due to almost 9% COV of the test results. This shows that designers and engineers will be more confident in using the guaranteed tensile-strength properties determined according to the CSA standard than the ASTM one. Moreover, it is important to note that the guaranteed tensile strength for the ASTM specimens is lower than the 655 MPa specified by ACI-440.6M (2008) for 20 mm diameter standard-modulus GFRP bars, when considering the outliers in the analysis. A total of 6 specimens (13%) out of 45 specimens are under this category.

Conclusions

Four independent laboratories were compared for their specimen preparation and tensile-test results for 19 mm diameter GFRP bars according to the provisions of ASTM

D7205 / D7205M-06 (2011) and CSA S806 (2012). Based on the results of testing a total of 85 tensile specimens in this study, the following conclusions were drawn:

- A steel tube filled with a cement grout provided effective anchorage at the ends of the FRP bars for tensile testing. A gauge length of not less than 40 times the bar diameter, as prescribed by the ASTM and CSA standards, was sufficient to obtain reliable tensile properties. Similarly, an anchor length of 460 mm or longer was acceptable to effectively transmit the tensile force from the grip to the bars. Using these specimen dimensions, all of tested GFRP bars failed within the gauge length with no slip observed in the anchor.
- The loading rate recommended by the ASTM and CSA standards had no significant effect on the measured tensile properties of the GFRP bars. All of the specimens tested failed within 3 min of load application. Nevertheless, a constant load rate (or strain rate) was preferred to constant cross-head speed for the tensile characterization of the FRP bars. As was found in this study, a constant cross-head speed does not guarantee a constant loading rate, especially near the test outset, which significantly affects the distribution of the measured tensile strength and MOE.
- The grout thickness between the outer surface of the bar and the inner wall of the tube had a significant effect on the measured tensile properties of the bars due to the exothermic reaction during grout curing. The specimens with a thick cement grout experienced a surface temperature higher than the bar’s T_g, which could potentially damage the bar surface. Up to 202°C was measured for 8.5 mm thick cement grout (prepared as per ASTM D7205, Annex A), while only 110°C for 6.5 mm thick grout (prepared as per CSA S806). Thus, it is recommended that the anchor should be chosen according to grout thickness rather than opting for a standard tube size.

- The tensile strength of the ASTM specimens was statistically different from the CSA specimens. The 10% lower average tensile strength of the ASTM specimens was due to the reduced bond between the fibers and resin, which resulted by the high temperature as the cement grout cured. This also resulted in a coefficient of variation of almost 16% for the ASTM specimens. Discarding the test outliers would give the ASTM specimens a tensile strength almost 4% lower and a COV of 5% compared to the CSA specimens.
- There was no statistically difference between the average MOE of the ASTM and CSA specimens. The wider variation in the MOE values obtained with ASTM D7205 was due to the location of the points in the stress–strain curve from which this property was calculated. Similarly, the strain interval in which the MOE was calculated for the ASTM specimens is shorter than for the CSA ones and it was located closer to the test outset, when the testing machine and its components may not be evenly acting on the specimen. A more consistent MOE was obtained at a higher load, i.e., between 25% and 50% of the ultimate, once the specimen and grips had settled properly during the test.
- The CSA method returned better repeatability than the ASTM one, as shown by the smaller dispersion of the tensile strength and MOE values. All the tested CSA specimens were within the ±10% of the mean tensile strength and MOE, and almost 90% were within ±5% of the mean tensile properties. On the other hand, there was a wide distribution in the tensile-strength values and MOE for the ASTM specimens, with 13% of the results significantly lower than the overall average tensile strength.
- The CSA specimens gave guaranteed tensile properties at least 7% higher than the ASTM specimens. When the outliers in the test results were considered in the

analysis, the guaranteed tensile strength for the ASTM specimens was lower than the values specified in ACI 440.6M.

Based on these conclusions, some amendments should be made to the ASTM D7205, Annex A method in order to effectively characterize the tensile properties of FRP bars. Based on our comparison, the CSA method yielded more reliable results than the ASTM one. Accordingly, the former was more effective and should be given preference, since the anchor can, in no way, make the GFRP bar appear stronger than it is. Moreover, a detailed chart of anchor size should be constructed solely as recommendations to facilitate testing of FRP bars. The appropriate anchor dimensions should be summed up as "*allowing the right amount of grout to be used and sufficiently long to achieve the accurate tensile strength of the specimen without slippage*" or "*those recommended by the manufacturer*."

Acknowledgments

This study was conducted with funding from the Natural Sciences and Engineering Research Council of Canada (NSERC) Research Chair in Innovative FRP Reinforcement for Concrete Infrastructure, the Fonds de recherche du Quebec en nature et technologie (FRQ-NT), and the Service des matériaux d'infrastructures of the Ministry of Transportation of Quebec. The authors wish to express their gratitude and appreciation to Pultrall Inc., Thetford Mines, Quebec, for material support. The technical assistance from the staff of the Structural Laboratory in the Department of Civil Engineering, Faculty of Engineering at the University of Sherbrooke is also acknowledged. The fourth author also acknowledges the scholarship granted by the Australian Government Endeavour Research Fellowships to undertake his research and professional development at the University of Sherbrooke.

References

American Concrete Institute (2008). Metric specification for carbon & glass fiber-reinforced polymer bar materials for concrete reinforcement. ACI-440.6M-08, Farmington Hills, Michigan, USA.

American Concrete Institute (2012). Guide test methods for fiber-reinforced polymer, ACI 440.3R-12, Farmington Hills, Michigan, USA.

American Concrete Institute (2015). Guide for the design and construction of concrete reinforced with FRP bars, ACI 440.1R-15, Farmington Hills, Michigan, USA.

Ahmed, E.A., El-Sayed, A.K., El-Salakawy, E., and Benmokrane, B. (2010). "Bend strength of FRP stirrups: Comparison and evaluation of testing methods." *Journal of Composites for Construction*, 14(1), 3-10.

ASTM Standard D570 − 98 (2010). Standard test method for water absorption of plastics. *ASTM D570 − 98,* ASTM International, West Conshohocken, Philadelphia, Pa 19103.

ASTM Standard D3171-15 (2015). Standard test methods for constituent content of composite materials. *ASTM D3171−15,* ASTM International, West Conshohocken, Philadelphia, Pa 19103.

ASTM Standard D5117-09 (2009). Standard test method for dye penetration of solid fiberglass reinforced pultruded stock. *ASTM D5117 − 09,* ASTM International, West Conshohocken, Philadelphia, Pa 19103.

ASTM Standard D7205 / D7205M-06 (2011). Standard test method for tensile properties of fiber reinforced polymer matrix composite bars. *ASTM D7205 / D7205M-06,* ASTM International, West Conshohocken, Philadelphia, Pa 19103.

ASTM E4 - 01 (2001). Standard practices for force verification of testing machines. *ASTM E4-01*, ASTM International, West Conshohocken, Philadelphia, Pa 19103.

ASTM Standard E1131-08(2014). Standard test method for compositional analysis by thermogravimetry. *ASTM E1131-08*, ASTM International, West Conshohocken, Philadelphia, Pa 19103.

ASTM Standard E1356-08(2014). Standard test method for assignment of the glass transition temperatures by differential scanning calorimetry. *ASTM E1356-08*, ASTM International, West Conshohocken, Philadelphia, Pa 19103.

Baninayat, P. and Patnaik, A. (2014). "Variability of mechanical properties of basalt fiber reinforced polymer bars manufactured by wet-layup method." *Materials and Design*, 56, 898-906.

Benmokrane, B., El-Salakawy, E., El-Ragaby, A., and Lackey, T. (2006). "Designing and testing of concrete bridge decks reinforced with glass FRP bars." *Journal of Bridge Engineering*, 11(2), 217-229.

Bouguerra, K., Ahmed, E.A, El-Gamal, S., and Benmokrane, B. (2011), "Testing of full-scale concrete bridge deck slabs reinforced with fibre-reinforced polymer (FRP) bars", *Construction and Building Materials*, 25, 3956-3965.

Canadian Standards Association (CSA). (2010). "Specification for fibre-reinforced polymers." CAN/CSA-S807, Rexdale, Ontario, Canada.

Canadian Standards Association (CSA). (2012). "Design and construction of building structures with fibre-reinforced polymers." CAN/CSA S806-12, Rexdale, Ontario, Canada.

Canadian Standards Association (CSA). (2006-Edition 2014). "Canadian highway bridge design code—Section 16, updated version for public review." CAN/CSA-S6-14, Rexdale, Ontario, Canada.

Carvelli, V., Giulia, F., and Pisani, M.A. "Anchor system for tension testing of large diameter GFRP bars." *Journal of Composites for Construction*, 13(5), 344-349.

Castro, P.F. and Carino, N.J. (1998). "Tensile and non-destructive testing of FRP bars." *Journal of Composites for Construction*, 2(1), 17-27.

Gentry, R., Bakis, C., Harries, K., Brown, J., Prota, A., and Parretti, R. (2012). "Development of ASTM test methods for FRP composite materials: Overview and transverse shear." *Proceedings of the* 6*th International Conference on FRP Composites in Civil Engineering (CICE 2012), Rome, Italy, 13-15 June 2012,* paper 12-513, 8 p.

IBM Corp. Released 2015. IBM SPSS Statistics for Windows, Version 23.0. Armonk, NY: IBM Corp.

International Standard ISO 10406-1 (2015). Fibre-reinforced polymer (FRP) reinforcement of concrete – Test methods, Part 1: FRP bars and grids. *ISO 10406-1:2015(E),* ISO, Geneva, Switzerland.

Kocaoz, S., Samaranayake, V.A., and Nanni, A. (2005). "Tensile characterization of glass FRP bars." *Composites: Part B,* 36, 127-134.

Li, G., Wu, J., and Ge, W. (2015). "Effect of loading rate and chemical corrosion on the mechanical properties of large diameter glass/basalt-glass FRP bars." *Construction and Building Materials,* 93, 1059-1066.

Malvar, L.J. (1995). "Tensile and bond properties of GFRP reinforcing bars." *ACI Materials Journal,* 92(3), 276-285.

Manalo, A.C., Benmokrane, B., Park, K., and Lutze, D. (2014). "Recent developments on FRP bars as internal reinforcement in concrete structures". *Concrete in Australia,* 40(2), 46-56.

Maranan, G. B., Manalo, A. C., Benmokrane, B., Karunasena W. M., and Mendis, P. (2015). "Evaluation of the flexural strength and serviceability of geopolymer concrete beams reinforced with glass-fibre-reinforced polymer (GFRP) bars". *Engineering Structures,* 101, 529-541.

Maranan, G. B., Manalo, A. C., Benmokrane, B., Karunasena W. M., and Mendis P. (2016). “Behavior of concentrically loaded geopolymer concrete columns reinforced longitudinally and transversely with GFRP bars”. *Engineering Structures*, 117, 422-436.

Micelli, F., and Nanni, A. (2004). “Durability of FRP rods for concrete structures.” *Construction and Building Materials,* 18, 491-503.

Portnov, G. and Bakis, C.E. (2008). “Analysis of stress concentration during tension of round pultruded composite rods.” *Composite Structures,* 83, 100-109.

Robert, M. and Benmokane, B. (2010). “Behaviour of GFRP reinforcing bars subjected to extreme temperatures.” *Journal of Composites for Construction,* 14(4), 353-360.

Roopa, T.S., Murthy, H.N., Sudarshan, K., Nandagopan, O.R., Kumar, A., Krishna, M., and Angadi, G. (2014). “Mechanical properties of vinylester/glass and polyester/glass composites fabricated by resin transfer molding and hand lay-up.” *Journal of Vinyl and Additive Technology,* 21(3), 166-174.

Schessar, D., Yang, Q.D., Nanni, A., and Giancaspro, J.W. (2014). “Expansive grout-based gripping systems for tensile testing of large-diameter composite bars.” *Journal of Materials in Civil Engineering,* 26(2), 250-258.

Tannous, F.E. and Saadatmanesh, H. (1998). “Environmental effects on the mechanical properties of E-glass FRP rebars.” *ACI Materials Journal*, 95(2), 87-100.

Wisnom, M.R. (1999). “Size effects in the testing of fibre-composite materials.” *Composites Science and Technology*, 59, 1937-1957.

Zhang, B., Benmokrane, B., Chennouf, A., Mukhopadhyaya, P., and El-Safty, A. (2001). “Tensile behaviour of FRP tendons for prestressed ground anchors.” *Journal of Composites for Construction,* 5(2), 85-93.

List of Tables

List of Figures

Table 1. Comparison between the ASTM and CSA standards for tensile testing

Test Standard	Preparation Method	Speed of Testing	MOE Calculation
ASTM D7205-06	Annex A	• Constant strain rate • Failure within 1 to 10 min or cross-head speed of 0.01 x free length/min	Between 0.1% and 0.3% of strain
CSA S806-12	Annex B	Constant stress rate of 250 to 500 MPa/min	Between 25% and 50% of the ultimate load

Table 2. Physical properties of the sand-coated No. 6 GFRP bars

Property	Test Method	Average	Std. Dev.
Actual diameter (mm)	CSA-S806, Annex A (2012)	19.67	0.08
Actual cross-sectional area (mm^2)	CSA-S806, Annex A (2012)	303.76	2.55
Fiber content by weight (%)	ASTM D3171-15 (2015)	82.7	0.2
Transverse CTE, ($x10^{-6}/^{o}C$)	ASTM E1131-08 (2014)	22.0	1.8
Void content (%)	ASTM D5117-09 (2009)	0	0
Water absorption at 24 h (%)	ASTM D570-98 (2010)	0.019	0.004
Water absorption at saturation (%)	ASTM D570-98 (2010)	0.039	0.010
Cure ratio (%)	ASTM E1356-08 (2014)	100	0
Tg (^{o}C)	ASTM E1356-08 (2014)	125.2	1.3

Table 3. Dimensions of tensile specimens prepared according to ASTM and CSA standards

Test Standard	**Outside Diameter (D_o), mm**	**Inside Diameter (D_i), mm**	**Anchor Length (L_a), mm**	**Gauge Length (L), mm**
ASTM D7205 Annex A	48	38	460	870
CSA S806 Annex B	42	32	675	760

Table 4. Description of the test machine and equipment at the 4 testing facilities

Laboratory	Test Machine	Acquisition Device	Cross-head Displacement Rate (mm/min)	Stress Rate (MPa/min)
A	Instron	Extensometer	8.7 (0)	300 (0)
B	Baldwin	LVDT	8.7 (0)	299 (0.2)
C	Riehle	Extensometer	8.6 (0.50)	310 (16.7)
D	Baldwin	LVDT	8.9 (2.76)	359 (46.3)

Table 5. Tensile strength in MPa of GFRP bars

	ASTM				CSA			
No.	A	B	C	D	A	B	C	D
1	933	929	879	821	916	899	919	895
2	855	835	461*	630*	907	940	924	910
3	929	880	915	448*	899	912	891	910
4	435*	825	863	809	845	908	896	851
5	886	899	910	852	922	942	916	888
6	836	877	906	772	894	905	899	887
7	885	896	886	861	860	927	927	917
8	856	890	844	861	899	922	918	835
9	876	853	674*	831	841	892	925	884
10	911	907	448*	866	920	857	874	905
11	843	--	822	796	--	--	--	--
12	--	--	810	890	--	--	--	--
Mean value, MPa	840.5	879.1	784.8	786.4	890.3	910.4	908.9	888.2
Standard deviation (SD), MPa	132.0	31.0	160.4	120.9	29.0	23.8	16.9	25.2
Coefficient of variation (COV), %	16.5	3.7	22.4	16.3	3.4	2.8	2.0	3.0
Mean value, MPa	819.8				899.4			
SD, MPa	130.8				26.5			
COV, %	16.0				2.9			
Mean value*, MPa	866.5							
SD*, MPa	38.8							
COV*, %	4.5							

Note: * indicates that the test-result outliers have been discarded from the analysis.

Table 6. Modulus of Elasticity in GPa of GFRP bars

No.	**ASTM**				**CSA**			
	A	B	C	D	A	B	C	D
1	53.63	52.28	57.45	57.46	62.22	51.92	59.37	58.05
2	57.21	51.51	57.64	56.95	55.54	52.86	56.81	56.26
3	58.12	51.49	57.64	56.59	60.64	52.11	57.19	56.97
4	53.61	48.61	56.36	57.77	59.25	52.94	58.66	56.98
5	77.35*	50.96	59.57	56.47	56.52	52.39	57.54	57.76
6	53.25	51.68	58.45	53.03	59.47	51.84	58.74	57.44
7	53.36	52.75	58.56	56.59	54.78	52.75	59.70	57.44
8	52.40	52.02	57.46	59.61	57.13	52.24	59.02	57.81
9	56.96	52.60	58.89	56.32	55.72	52.27	58.66	56.90
10	47.42*	50.99	58.29	59.43	55.02	52.63	58.22	56.97
11	45.01*	--	57.89	58.17	--	--	--	--
12	--	--	59.12	58.17	--	--	--	--
Mean value, GPa	55.30	51.49	58.11	57.21	57.63	52.39	58.39	57.26
SD, GPa	8.31	1.18	0.86	1.78	2.60	0.39	0.94	0.54
COV, %	15.03	2.30	1.48	3.10	4.50	0.74	1.62	0.94
Mean value, GPa	55.71				56.42			
SD, GPa	4.82				2.75			
COV, %	8.64				4.88			
Mean value*, GPa	55.82							
SD*, GPa	2.82							
COV*, %	5.05							

Note: * indicates that the test-result outliers have been discarded from the analysis.

Table 7. Actual loading rate for tensile tests

Laboratory	**ASTM D7205 Specimens**			**CSA S806 Specimens**		
	Start	**End**	**Average**	**Start**	**End**	**Average**
Load rate between 0.1 and 0.3% of strain						
A	357 (10.0)	357 (7.6)	357 (7.9)	300 (0.6)	300 (0.3)	300 (0.3)
B	215 (9.1)	295 (6.1)	261 (2.9)	313 (2.8)	302 (1.2)	305 (0.9)
C	284 (24.1)	309 (26.2)	297 (24.2)	233 (17.4)	269 (15.8)	256 (16.2)
D	232 (114.9)	309 (90.6)	272 (102.3)	270 (31.5)	339 (62.3)	307 (34.1)
Load rate between 25% and 50% of the ultimate load						
A	369 (5.1)	359 (4.5)	365 (3.9)	300 (0.2)	300 (0.2)	300 (0)
B	321 (3.7)	335 (3.0)	330 (3.4)	299 (0.7)	299 (0.8)	299 (0.2)
C	320 (16.3)	352 (59.9)	331 (22.4)	292 (24.1)	319 (22.5)	310 (16.7)
D	323 (68.4)	308 (32.3)	307 (38.7)	359 (51.3)	348 (47.5)	359 (46.3)

Table 8. Actual and predicted tensile properties of 19 mm diameter GFRP bars

Properties	Materials (Roopa et al. 2014)		GFRP Bar, P_{bar}		
			Predicted	Actual	
	Glass fibers, P_f	Vinyl-ester resin, P_m		ASTM	CSA
Strength, MPa	2000	60	1553.8	819.8	899.4
MOE, GPa	70	3	54.6	55.7	56.4

Table 9. Independent samples *t*-test on tensile strength

Group Statistics

Method	*N*	*Mean*	*Std. Deviation*	*Std. Error Mean*
ASTM	45	819.80	130.84	19.50
CSA	40	899.45	26.52	4.19

Independent Samples Test

	Levene's Test for Equality of Variances		t-*test for Equality of means*						
								95% Confidence Interval of Difference	
	F	*Sig.*	*t*	*df*	*Sig. (2-tailed)*	*Mean Diff.*	*Std. Error Diff.*	*Lower*	*Upper*
Equal variances assumed	16.91	.000	-3.78	83	0.000	-79.65	21.07	-121.56	-37.73
Equal variances not assumed			-3.99	48.04	0.000	-79.65	19.94	-119.76	-39.54

Table 10. One-way ANOVA on tensile strength

Descriptive Table - ANOVA on tensile test

	Sum of Squares	*df*	*Mean Square*	*F*	*Sig.*
ASTM					
Between groups	67902.99	3	22634.33	1.354	0.270
Within groups	685306.21	41	16714.78		
Total	753209.20	44			
CSA					
Between groups	4194.90	3	1398.30	1.354	0.109
Within groups	23229.00	36	645.25		
Total	27423.90	39			

Tukey's HSD Post Hoc multiple comparisons on tensile strength

					95% Confidence Interval	
Lab	*Lab*	*Mean Difference*	*Std. Error*	*Sig.*	*Lower Bound*	*Upper Bound*
ASTM						
A	B	-38.64	56.48	0.903	-189.90	112.61
	C	55.62	53.96	0.733	-88.88	200.12
	D	54.03	53.96	0.749	-90.46	198.54
B	A	38.64	56.48	0.903	-112.61	189.90
	C	94.26	55.35	0.335	-53.95	242.49
	D	92.68	55.35	0.350	-55.54	240.91
C	A	-55.62	53.96	0.733	-200.12	88.88
	B	-94.26	55.35	0.335	-242.49	53.95
	D	-1.58	52.78	1.000	-142.91	139.74
D	A	-54.03	53.96	0.749	-198.54	90.46
	B	-92.68	55.35	0.350	-240.90	55.54
	C	1.58	52.78	1.000	-139.74	142.91
CSA						
A	B	-20.10	11.36	0.304	-50.69	10.49
	C	-18.60	11.36	0.371	-49.19	11.99
	D	2.10	11.36	0.998	-28.49	32.69
B	A	20.10	11.36	0.304	-10.49	50.69
	C	1.50	11.36	0.999	-29.09	32.09
	D	22.2	11.36	0.224	-8.39	52.79
C	A	18.60	11.36	0.371	-11.99	49.19
	B	-1.50	11.36	0.999	-32.09	29.09
	D	20.70	11.36	0.280	-9.89	51.29
D	A	-2.10	11.36	0.998	-32.69	28.49
	B	-22.20	11.36	0.224	-52.79	8.39
	C	-20.70	11.36	0.280	-51.29	9.89

Table 11. Independent samples *t*-test on MOE

Group Statistics

Method	*N*	*Mean*	*Std. Deviation*	*Std. Error Mean*
ASTM	45	55.71	4.81	0.71
CSA	40	56.41	2.75	0.43

Independent Samples Test

	Levene's Test for Equality of Variances		*t-test for Equality of means*						
								95% Confidence Interval of Difference	
	F	*Sig.*	*t*	*df*	*Sig. (2-tailed)*	*Mean Diff.*	*Std. Error Diff.*	*Lower*	*Upper*
Equal variances assumed	3.81	.054	-0.81	83	.418	-0.70	0.86	-2.42	1.01
Equal variances not assumed			-0.83	71.38	.405	-0.70	0.84	-2.37	0.97

Table 12. One-way ANOVA on MOE

Descriptive Table - ANOVA on MOE

	Sum of Squares	*df*	*Mean Square*	*F*	*Sig.*
Between groups	476.57	3	158.85	15.140	.000
Within groups	849.86	81	10.49		
Total	1326.43	84			

Tukey’S HSD Post Hoc multiple comparisons on MOE

Lab	*Lab*	*Mean Difference*	*Std. Error*	*Sig.*	*95% Confidence Interval*	
					Lower Bound	*Upper Bound*
A	B	4.46	1.01	0.000	1.81	7.12
	C	-1.82	0.98	0.258	-4.41	0.76
	D	-0.82	0.98	0.839	-3.41	1.76
B	A	-4.46	1.01	0.000	-7.12	-1.81
	C	-6.29	1.00	0.000	-8.92	-3.67
	D	-5.29	1.00	0.000	-7.91	-2.66
C	A	1.82	0.98	0.258	-0.76	4.42
	B	6.29	1.00	0.000	3.67	8.92
	D	1.00	0.97	0.733	-1.55	3.56
D	A	0.82	0.98	0.839	-1.76	3.41
	B	5.29	1.00	0.000	2.66	7.91
	C	-1.00	0.97	0.733	-3.56	1.55

Table 13. Guaranteed tensile properties for 19 mm sand-coated GFRP bars

	ACI440.1R-06			**CSA S807-10**			
Guaranteed tensile strength							
Method	**$f_{u,ave}$ (MPa)**	**σ (MPa)**	**f^*_{fu} (MPa)**	**COV (%)**	**n**	**F_{t_CSA}**	**f^*_{fu} (MPa)**
ASTM	819.8	130.8	427.9	16.0	45	0.71	581.8
ASTM*	866.5	38.9	749.8	4.5	39	0.91	793.2
CSA	899.4	26.5	819.9	2.9	40	0.94	849.3
Design MOE							
Method	**$E_{u,ave}$ (GPa)**	**σ (GPa)**	**E_f (GPa)**	**COV (%)**	**n**	**F_{E_CSA}**	**E_f (GPa)**
ASTM	55.7	4.8	55.7	8.6	45	0.84	46.8
CSA	56.4	2.8	56.4	4.9	40	--	56.4

Note: * indicates that the test-result outliers have been discarded from the analysis.

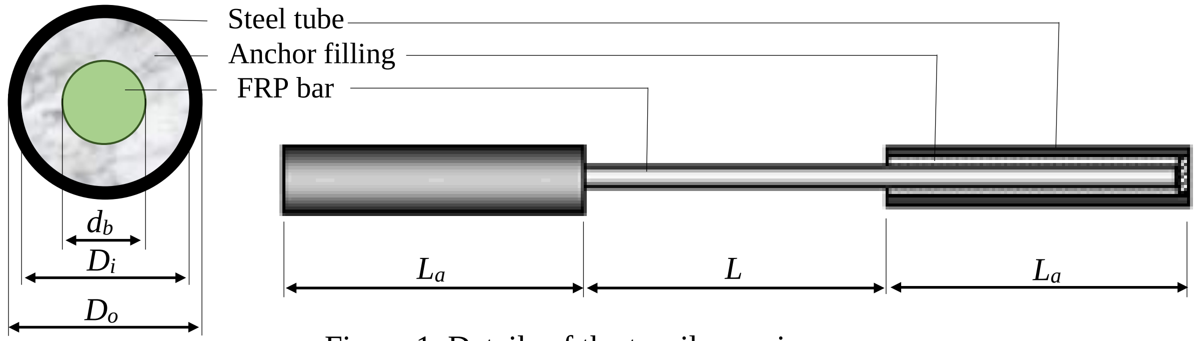

Figure 1. Details of the tensile specimens

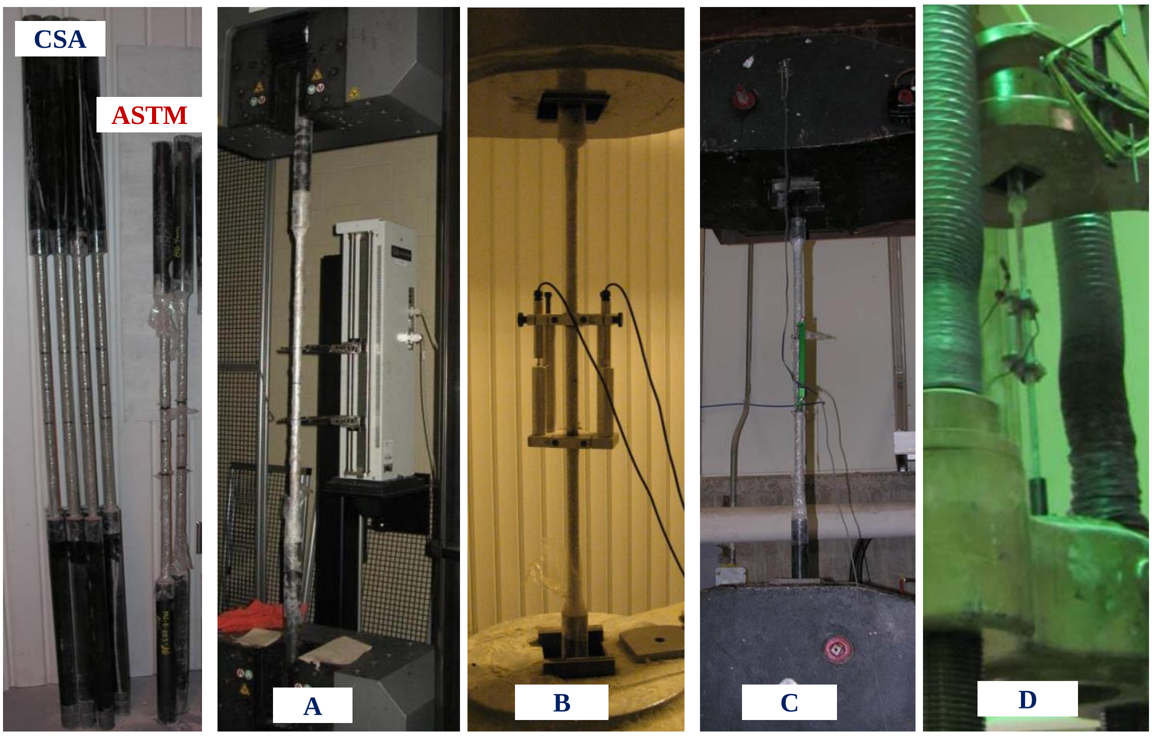

(a) Specimens (b) Test setup (Laboratories A, B, C, and D)

Figure 2. Actual specimens and test setup

Figure 3. Failure of tensile specimens

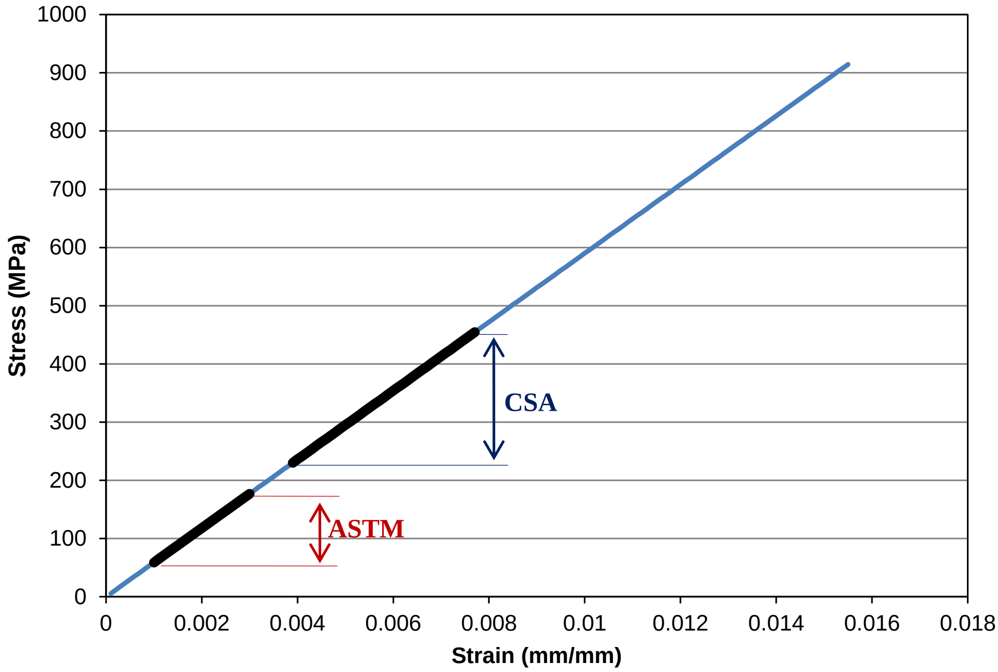

Figure 4. Typical stress–strain behavior of GFRP bars

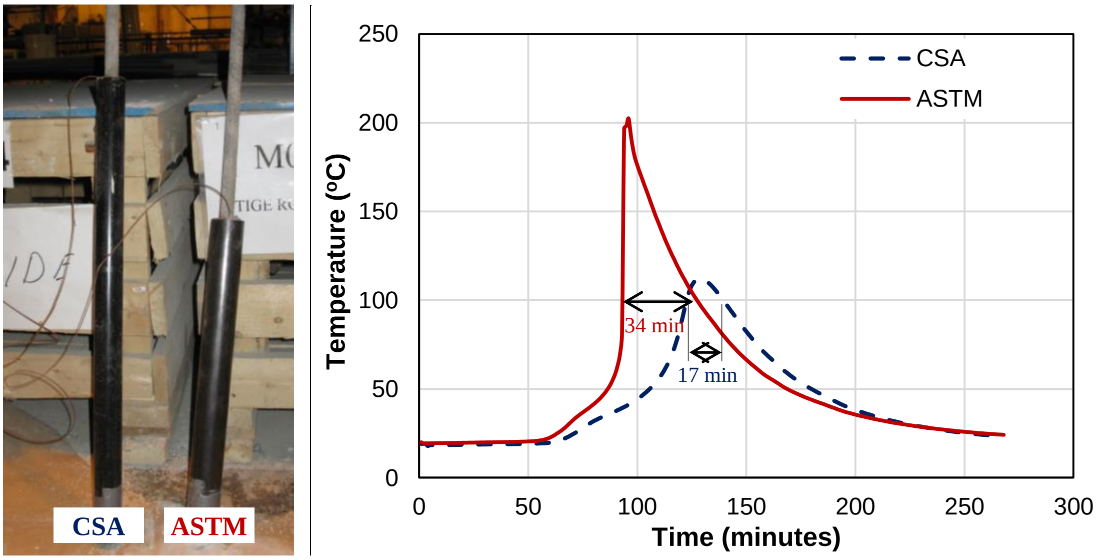

Figure 5. Temperature of the grout in the anchor

(a) ASTM specimens

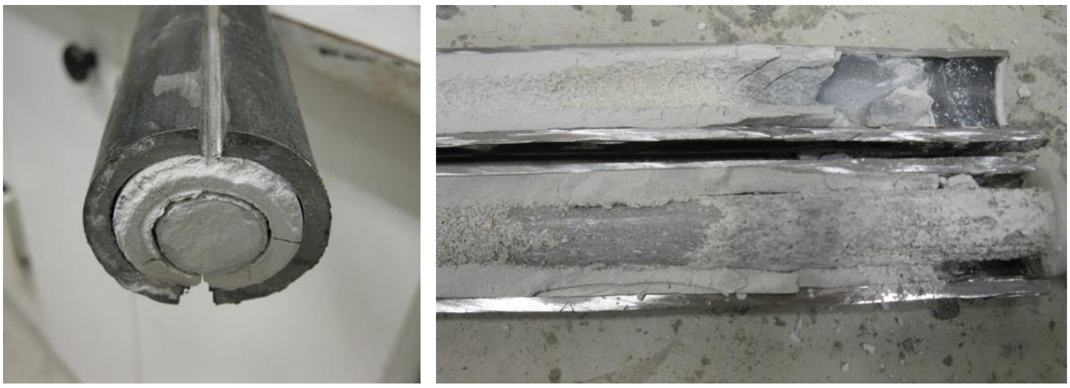

(b) CSA specimens

Figure 6. Condition of the bar ends in the steel anchor

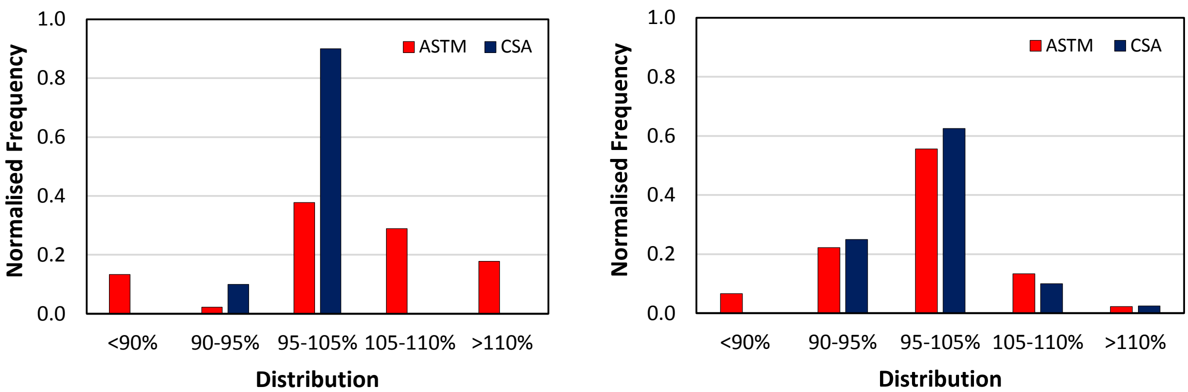

(a) Tensile strength (b) MOE

Figure 7. Distribution of tensile properties